Advanced Course and Workshop on Blood Flow
BF 2005 – (pp.109–134) – Warsaw, 2005.

Experimental Assessment of Wall Shear Flow

Ulrich Kertzscher, Perrine Debaene,
Leonid Goubergrits, and Klaus Affeld

Biofluidmechanics Laboratory
Charité, Universitätsmedizin Berlin
Spandauer Damm 130
14050 Berlin
Germany
ulrich.kertzscher@charite.de

The assessment of wall shear flow is of interest for different technical and scientific fields. One of the research fields is biofluidmechanics, where a close relationship is assumed between flow and biological phenomena. Special problems are encountered when assessing the wall shear flow in biofluidmechanics. The flow is often pulsatile, the walls are curved and even vaulted, sometimes the walls are flexible and the wall shear flow should also be assessed with a high spatial and temporal resolution.
An overview is given about existing methods to assess the wall shear flow. Some of these methods are point methods, others obtain a field. All of these methods have special advantages but also drawbacks. We therefore developed a new measurement method to investigate the flow close to a wall. This method is applicable at curved and vaulted walls, in unsteady flows, is non-intrusive, and obtains flow fields with spatial and temporal resolution.
The new method was validated in a steady and unsteady laminar flow in a rectangular duct and in a rectangular U-shaped duct with a backward facing step. The last validation step was in an U-shaped duct with a lenticular cross section and a backward facing step. The results correspond closely with either the analytical or the numerical solution.

1. Introduction

The assessment of wall shear flow is interesting for different technical and scientific fields. Examples are: removal of biofilms in medicine, cleaning of containers, cultivation of shear sensitive cells and development and research in the field of biofluidmechanics. The latter comprises of the development of blood pumps and artificial vessels as well as atherogenisis.

In 1856 Rudolf Virchow postulated the interaction between flow, blood and walls. This interaction is known as Virchow's Triad. It has often been proven qualitatively by researchers.

It is known that there is a close relationship between flow and biological phenomena, for instance thrombus formation [9] or atherosclerotic events [1]. In particular, the wall shear stress plays a role because it influences the structure and function of the endothelial cells [10] as well as the behaviour of platelets [6]. An example for a thrombus formation at an artificial heart valve and an example for the development of atherosclerosis, here at a carotid bifurcation, are shown in Fig. 1. However, quantification of the influence of flow parameters like wall shear stress on the wall is still lacking.

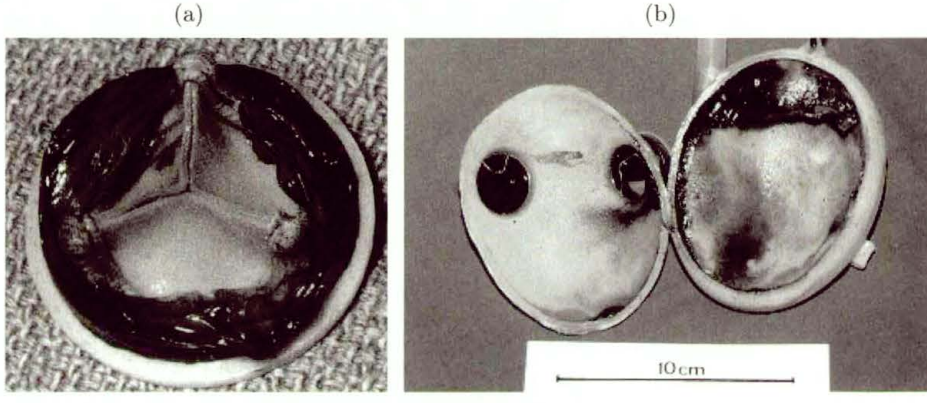

FIGURE 1. (a) Thrombus generation at an artificial heart valve [11], (b) Development of atherosclerotic lesions in a carotid bifurcation

The measurement of the flow close to the wall, especially of the wall shear stress, is a precondition to our understanding of atherosclerotic events and also our ability to avoid thrombus generation in artificial organs. Nevertheless this is a challenging experimental problem. Reasons for this are the pulsatile flow, the curved or vaulted as well as flexible walls, and, depending on the model, the small diameter. In addition one is interested in assessing the wall shear flow with high spatial and temporal resolution.

In Sec. 2 an overview is given about existing methods to assess the wall shear flow. In Sec. 3 a new method is presented to assess the wall shear flow including the wall shear stress.

2. Existing Methods to Assess the Wall Shear Flow

Many methods to assess the wall shear flow and wall shear stress exist. They can be divided into point or field methods.

2.1. Point Methods

Point methods yield the flow properties at the wall only at one point. Some of the point methods can be extended to field methods by using an array of probes. It is possible to extend the methods explained later with a hot wire and a surface fence, especially in the case of micro-electro-mechanical-systems. The disadvantages of the basic method are kept.

2.1.1. Preston tube. The Preston tube is a modified Pitot tube and measures the pressure profile p near the wall, Fig. 2. It is possible, from this profile, to calculate the velocity profile close to the wall and to calculate with Newton's equation the wall shear stress:

$$\tau_w = \eta \frac{\partial v}{\partial y}\Big|_w . \tag{2.1}$$

In this equation the wall shear stress τ_w is equal to the dynamic viscosity η multiplied with the velocity gradient at the wall. This method is quite invasive and not very accurate.

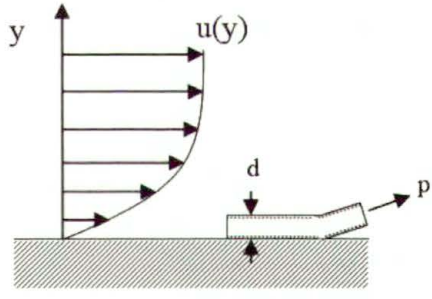

FIGURE 2. Preston tube

2.1.2. Surface hot films. A hot film element is introduced into the wall (Fig. 3). It should be flush with the wall and electrically heatable. The heat

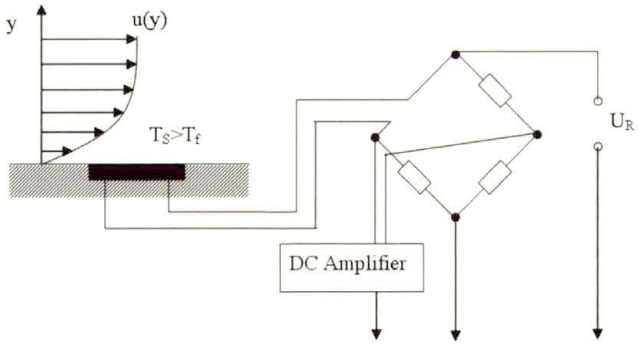

FIGURE 3. Surface hot film (T_s: Temperature of the hot film; T_f: Temperature of the fluid)

loss of the element is a measure for the velocity of the fluid close to the wall. From this velocity, the wall shear stress can be calculated. This method is almost non invasive and may be used to assess the mean wall shear stress. Problems arise if the temperature of the fluid is not constant. The heat loss in the wall has to be accounted for and a calibration procedure is always necessary.

2.1.3. Wall-fixed hot wire and pulsed hot wire. The principle of the wall-fixed hot wire is similar to the hot film measurements in the section before. Instead of a hot film, a hot wire with a small diameter is used and fixed close to the wall (Fig. 4). The heat loss of the hot wire is proportional to the velocity of the fluid. If the hot wire is close enough to the wall you

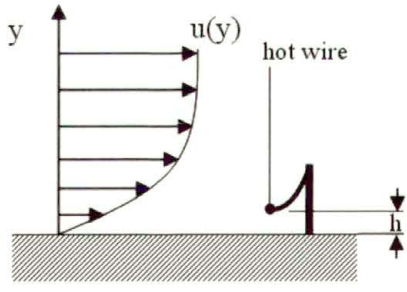

FIGURE 4. Wall-fixed hot wire

are able to calculate the wall shear stress from this velocity. In other words, the hot wire has to be in the viscous sublayer, where the velocity profile is linear. It is then possible to use Newton's equation (2.1). This method has to be calibrated before each measurement and just as for hot films you have to consider a temperature change in the fluid. This method is quite invasive. Quite similar to the hot wire method is the pulsed hot wire method: a hot wire is heated for a short period and the released heat is measured by a second hot wire further downstream. It is possible to assess the velocity from the distance and the time lag. Aside from the problems of the hot wire you have to account for the diffusion of heat. The heat cloud is not only transported by convection but also by diffusion.

2.1.4. Surface fence in the sublayer. The pressure loss is measured over a surface fence with the height h, Fig. 5. It is possible to calculate the velocity and the wall shear stress from the pressure difference before and after the fence. This method is very good in order to measure the time resolved shear stress if the fence is in the linear part of the velocity field, but is invasive and quite error-prone. Errors can be caused by a pressure gradient in the flow, imperfections of the fence or a blockage of the pressure ports.

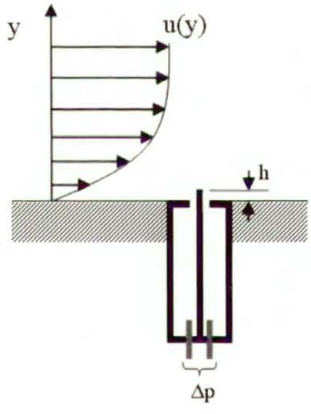

FIGURE 5. Surface fence

2.1.5. Laser Doppler velocimetry (LDV). This is a widely used non invasive method to measure the fluid velocity in one point. In the easiest case two laser beams with the same wave length are crossed, see Fig. 6. A mea-

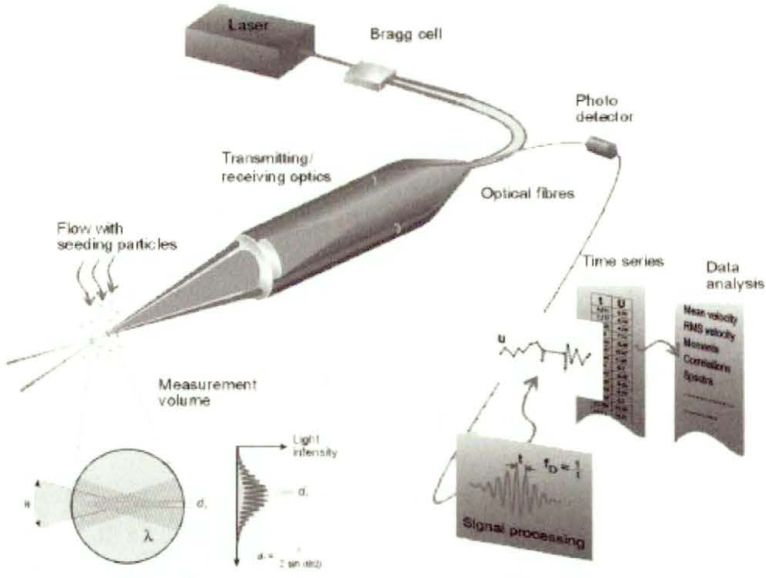

FIGURE 6. Laser Doppler velocimetry [4]

surement volume is defined by the two crossing laser beams. A fringe pattern which is caused by interference is visible in this volume. Tracer particles are added to the fluid. A tracer particle passing the measurement volume and therefore this fringe pattern, emits light with a frequency which depends upon the velocity of the particle. It is therefore possible to measure a velocity profile and to calculate the wall shear stress. This method has a high spatial and time resolution and it is not necessary to calibrate the system. This system can detect the flow direction when introducing a Bragg cell, which causes a defined frequency shift between the two laser beams. It is only a point method and the measurement of velocity fields is time consuming. Measurements in unsteady flows can be difficult.

2.2. Field Methods

Field methods yield the flow properties at the wall in an area.

2.2.1. Oil film interferometry. Small oil drops or a very thin oil film is distributed on the wall. After a certain amount of time in a steady flow, an oil wedge can be seen, Fig. 7. The distribution of the thickness of the oil can be measured by interferometry and is a measure of the wall shear stress.

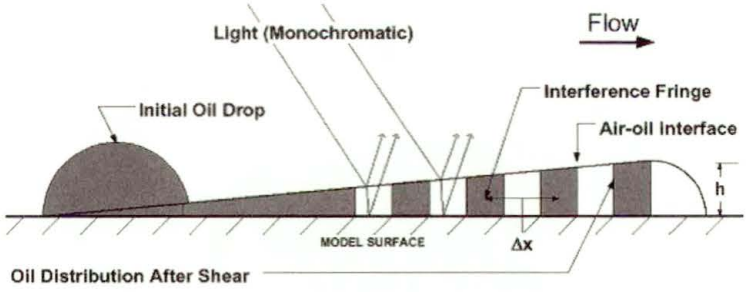

FIGURE 7. Oil film interferometry [16]

Some researchers tried to use this method in unsteady flows and to calculate the unsteady wall shear stress from the development of the oil wedge but to the knowledge of the authors their success was limited. The method is temperature dependent and it is usually necessary to calibrate the system.

2.2.2. Pressure sensitive paint. The pressure sensitive paint is distributed on the wall, see Fig. 8. The color change caused by pressure changes is recorded and it is possible to calculate the wall shear distribution after calibration. This is a method with a good resolution in time and space but it is not very sensitive and only applicable for higher pressures. Besides, the method is quite time and cost consuming.

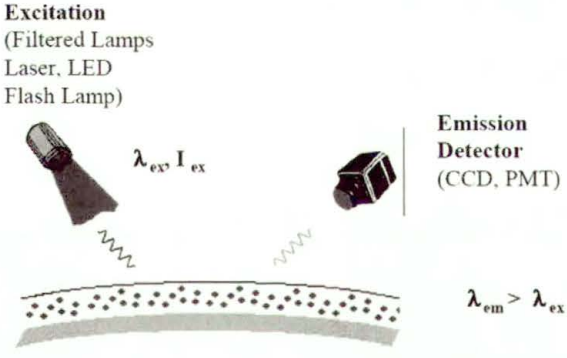

FIGURE 8. Pressure sensitive paint [2]

2.2.3. Paint erosion method. A water based colour-binder mixture is distributed on the wall. The erosion of the color is a qualitative measure of

the mean wall shear stress distribution. A quantitative analysis is theoretically possible and was investigated by our group. Figure 9 depicts the paint distribution after a certain amount of time in a stagnation point flow.

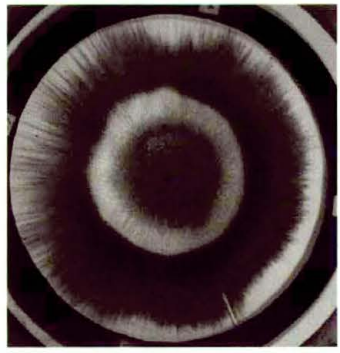

FIGURE 9. Paint distribution in a stagnation point flow

2.2.4. Laser photochromic velocimetry. A photochromic color is mixed into the fluid. This colour is completely transparent when illuminated with normal light, but visible if activated by ultraviolet light. Laser light is used to produce a regular coloured pattern in the fluid, for example, a grid pattern as can be seen in Fig. 10. This grid pattern is deformed under the influence of the flow. It is possible to calculate the velocity field in the volume from the recorded deformation of the pattern. In principle, it is possible to calculate the wall shear stress from the velocity field but the accuracy is limited. It is not easy to know the exact distance between the wall and a certain color point. Aside from this the method is more or less a procedure to assess the wall flow in a line.

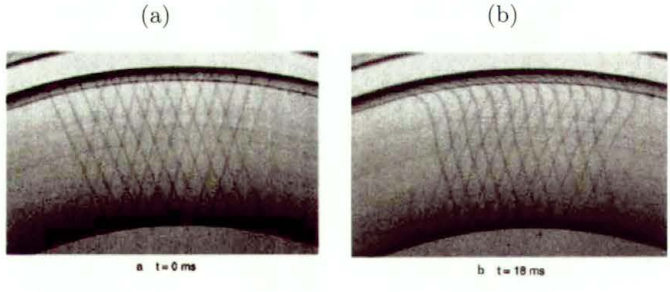

FIGURE 10. Deformation of a grid of photochromatic color under the influence of flow [12]

2.2.5. Particle image velocimetry (PIV). The basic idea of this powerful technique: tracer particles are mixed with the fluid and illuminated. By recording the position of the particles at two different points in time it is possible to assess the velocity of the particles through their displacement. In particle tracking velocimetry, every particle is considered. This method is limited to a certain seeding density. In PIV the flow is illuminated by a light sheet, see Fig. 11. The movement of the particles in the light sheet is recorded. The light sheet is divided into small interrogation areas and the movement of all particles within the interrogation area is evaluated by a correlation method. This method can be used to measure the velocity close to the wall. Unfortunately some problems arise there: distortion and deflection can occur at the wall because of the different refraction indices of the fluid and the wall. It is not easy to define the exact distance of the first measurement point to the wall.

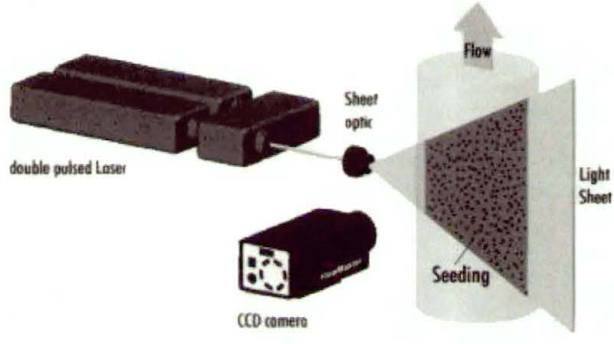

FIGURE 11. Particle image velocimetry [7]

2.2.6. 3D Scanning PIV. Multiple light sheets are produced with a rotating polygon mirror and a PIV analysis can be done in every individual light sheet (Fig. 12). If the light sheet is recorded from two directions, all three velocity components can be assessed in every light sheet. If the light sheets are quite close to each other this method can be considered three dimensional. This method is more or less limited to slower flows; the scanning velocity must be high enough. It is possible to produce the light sheets close to the wall and therefore calculate the wall shear stress field, but the resolution is limited by the thickness of the light sheet. This method is not applicable at vaulted walls.

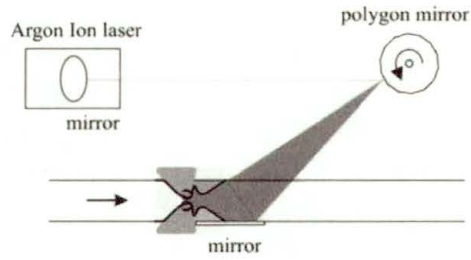

FIGURE 12. 3D Scanning PIV [15]

2.2.7. Holographic PIV. Another very interesting extension of the basic PIV idea is the holographic PIV, see Fig. 13. All particles in a volume are illuminated by diffusive laser light. These particles scatter the laser light which interferes with the light of a reference beam and is recorded by a holographic film. The volume information is divided into different layers and a PIV analysis is done for each layer. With this powerful technique it is, in principle, possible to measure the velocity close to the wall as a time resolved field. Until now, this method is very complex, time consuming and costly. For example, it is not easy to handle the enormous amount of data (about 100 Gigabyte per hologram).

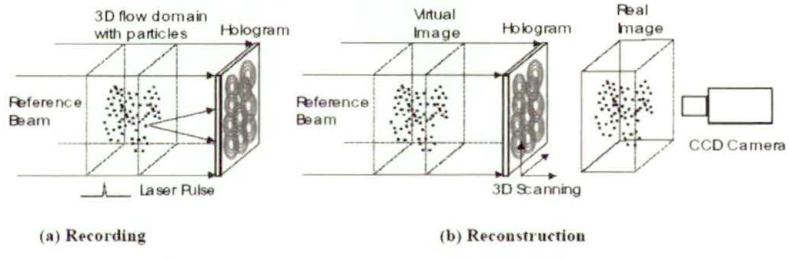

FIGURE 13. Holographic PIV [8]

2.2.8. Laser light sheet tomography. Similar to 3D Scanning PIV is the multicolour laser light sheet tomography. Many different colours are produced through mixing different laser colours. As a result, the particles in each layer are color coded. The layers may be as thin as 30 µm and it is possible to put the layers very close to each other. It is therefore possible to get a good spatial resolution close to the wall. Until now, the system is validated only

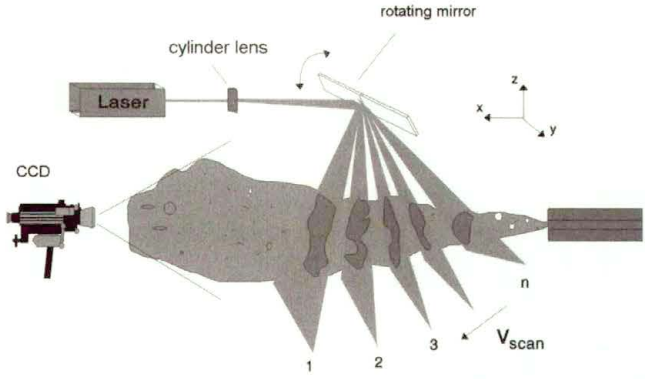

FIGURE 14. Laser light sheet tomography [13]

for gases, it is under development for fluids. Since the system works with light sheets it is possible to work with curved walls but not with vaulted.

2.3. Miscellaneous Methods

2.3.1. Ultrasonic Doppler method. Another possible use of the Doppler effect is ultrasound, see Fig. 15. The ultrasound wave is reflected by particles in the flow. The Doppler effect shifts the frequency of the incoming wave. This shift is a measure for the velocity in the direction of the ultrasound. With the use of a pulsed ultrasound it is possible to combine information about the frequency shift and the distance of the particle, which causes the shift. It is therefore possible to measure the velocity profile along a line. With this method only one component of the velocity is measured and only at two points close to the wall.

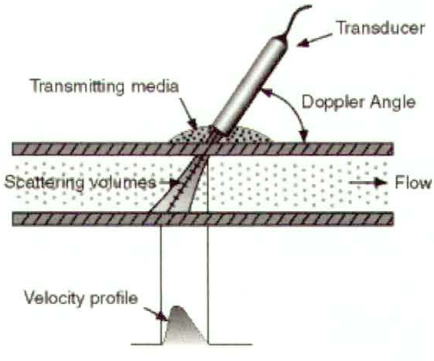

FIGURE 15. Ultrasonic Doppler method [14]

2.3.2. Laser Doppler profile sensor. With this highly sophisticated system it is possible to determine the position of a particle in the measuring volume of a LDV-system and to record the measuring signal from this particle. The distance of the particle to the wall is determined with the position. As a result, it is possible to measure a velocity profile in the wall vicinity with a very high precision. This method is very time consuming, costly and more or less a point measurement method.

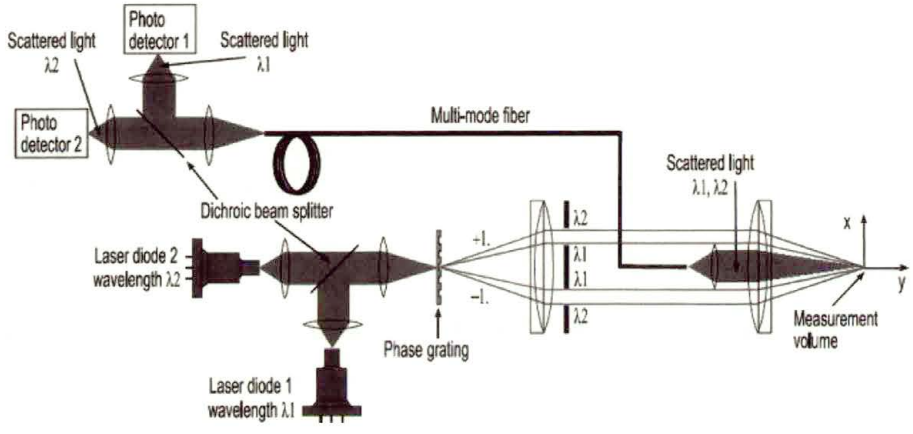

FIGURE 16. Laser Doppler profile sensor [3]

3. The New Method to Assess the Wall Shear Flow

All the methods in Sec. 2 have special advantages and disadvantages. Due to the problems in biofluidmechanics mentioned earlier, all the methods are of limited use. We therefore developed a new method with the following aims:

- noninvasive,
- determination of magnitude, direction and wall distance of the velocity field close to the wall,
- usable in unsteady flows,
- usable at curved and vaulted surfaces,
- easy to use, not too expensive.

3.1. Basic Idea and Realization of the New Method

As in conventional PIV, the new method is based on the observation and the digital recording of small, buoyant, light reflecting particles suspended in the fluid. Hence it is a particle image interrogation method. In the conventional 2D-PIV or PTV, a light sheet illuminates a plane in the flow. The particles in this plane light up and become visible. In the new method presented here, the whole flow near the wall is illuminated and all particles near the wall become visible. The transparent flow model is illuminated from the outside with monochromatic diffuse light. A dye is added to the fluid, which limits the penetration depth of the light into the flow model, see Fig. 17. According to optical laws, the penetration depth decreases if the concentration of the dye increases. Within the illuminated layer, the particles appear more or less bright, depending on their normal distance d_p to the wall. Particles near the wall appear brighter, i. e. have a higher gray value, than particles farther from the wall, see Fig. 18.

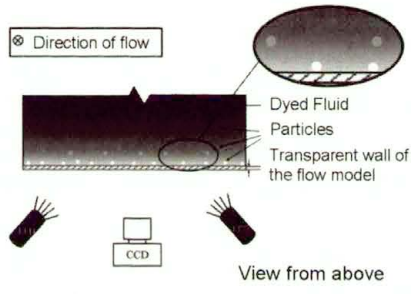

FIGURE 17. Basic principle of the new method

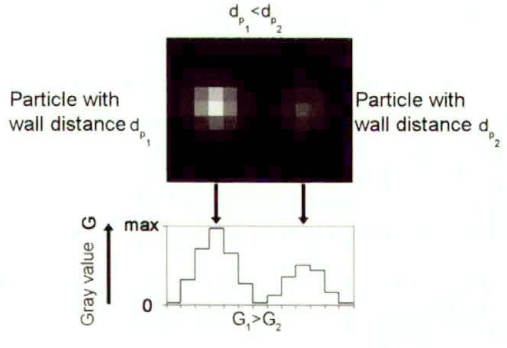

FIGURE 18. Gray value (G) of particles with different distances to the wall

An image processing leads to a separation of the near-wall flow into several layers. All the particles moving in one layer have the same gray value and, therefore, the same normal distance dp to the wall. For each layer, the motion of the particles can be determined with a conventional PIV algorithm — either cross correlation or particle tracking, depending on the number of particles in the plane. This results in a vector field for each layer. If the concentration of the dye, the lighting and the size of the particles are properly chosen, the particles closest to the wall are within the laminar sub-layer. This permits the calculation of the wall shear stress τ_w according to Eq. (2.1). A vector field of the wall shear stress results.

As for conventional PIV, the particles for the new method have to be neutrally buoyant, they should not alter the flow and should not interact with each other. The tracer particles should have additional properties as well. They should be spherical and monodisperse, otherwise it is impossible to calculate the right wall distance. Moreover, the particles should reflect the light more efficiently than the usual PIV tracer particles because of the absorption of the emitted and of the reflected light in the dyed fluid.

Special particles were developed according to the above-mentioned requirements. Encapsulated alginate beads with glass hollow micro-spheres were manufactured by LUM GmbH (Germany). The beads were prepared with the vibrating nozzle technique, using an encapsulation device (Inotech Encapsulation, Switzerland) based on laminar jet break-up. The particles have a mean diameter of 350 µm with a standard deviation smaller than 3% [5] and a density of ca. $1\,\mathrm{g\,cm^{-3}}$. The glass micro-spheres allow a density fitting of the beads and a good light scattering. These particles are large compared to particles used for conventional PIV, see section discussion.

Fluid, lighting and recording technique are interdependent, and have to be chosen so that the light absorption is sufficient, well defined and easily calculable. Furthermore, the lighting and recording techniques should be optimized, especially because the light amount reflected by the particles is quite small. We made use of a high-speed video camera having a resolution of 512×480 pixel at 250 fps (Fastcam Super 10 K, Roper Scientific MASD, USA). Sequences with max. 546 pictures can be recorded and saved instantaneously. The camera shows a maximum sensitivity at ca. 630–660 nm. To optimize the quality of the recording technique, these characteristics had been taken into account when choosing the light source. The bandwidth of the wavelength of the spectral distribution should not be larger than the

range of absorption of the dye. We used a diffuse light source composed of more than 60 red ultra bright Light Emitting Diodes (LED) (HLMP-ED31-SV000, Agilent Technologies Inc, USA). They have a dominant wavelength at 639 nm and a spectral halfwidth of 17 nm. Depending on the experiment and the velocity range we wanted to reach, we used water, or a mix of water and glycerin as an experimental fluid. A common blue food color named Patent Blue V (EEC Number: E131, Schuman und Sohn, Germany) was added to the fluid. This substance has a maximum absorption at 638 nm in water at pH= 5. The choice of this dye is based on two assumptions. First, the light absorption has to be optimized. This means that the absorption bands of the dye should be within the range of the dominant wavelengths of the LEDs. Furthermore, the absorption properties of the dye should be well defined and describable using common optical laws. Thus, it should be possible to calculate the maximal penetration depth of the light into the model according to the Beer Lambert law. The use of Patent Blue V fulfils both conditions.

3.2. Determination of the Particle-Wall Distance

The assessment of the relationship between the gray value of a particle and its distance from the wall is the foundation for the separation of the particles into different layers. To associate each gray value to a wall distance, a calibrating measurement was necessary. Particles in the fluid were moved in small steps from the wall. With our high speed camera the gray value was observed for every step. In Fig. 19 the result of such a calibration measurement is depicted. This calibration has to be done every time a fluid with a new colour concentration is used.

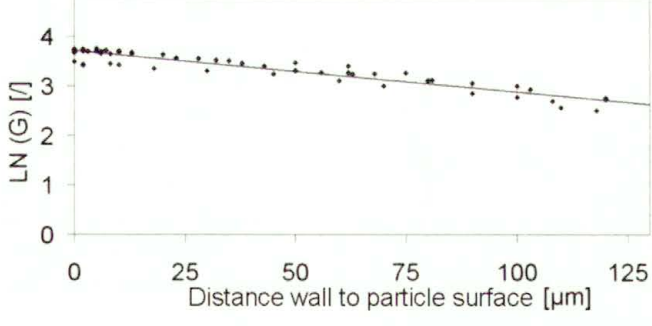

FIGURE 19. Observed gray value (G) depending on the particle distance to the wall

3.3. Validation of the New Method

The validation process was done in different steps. First, the validation was done using steady and pulsatile flows at planar walls. The next step was an investigation at planar walls with a complex steady flow. The last validation step used complex, steady flow at vaulted walls. The validation process is summarized in Fig. 20.

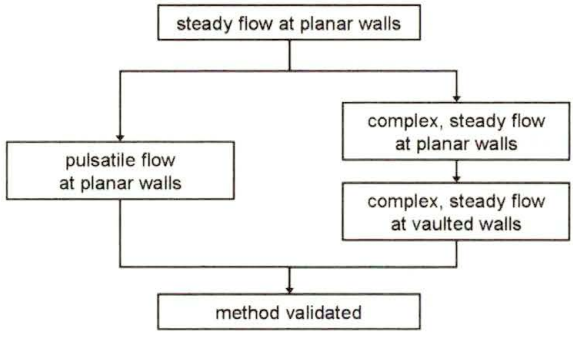

FIGURE 20. Validation of the new method

3.3.1. Validation in a steady flow at planar walls. As a steady flow at planar walls we have chosen a steady, laminar flow in a straight duct with a rectangular cross section. In Fig. 21 the dimensions of the duct and the well

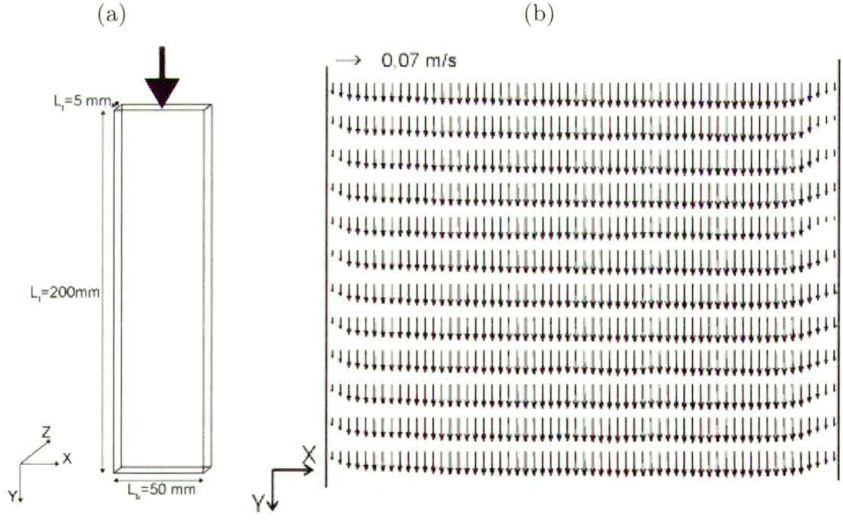

FIGURE 21. Rectangular duct and measured velocity field close to the wall

known velocity field close to the wall are depicted. The acquired experimental values of the velocity close to the wall were compared to the values of the analytical solution. The difference is about 10%.

3.3.2. Validation in a pulsatile flow at planar walls. For this validation step the same duct as before was investigated, but with a pulsatile flow. The flow curve is depicted in Fig. 22.

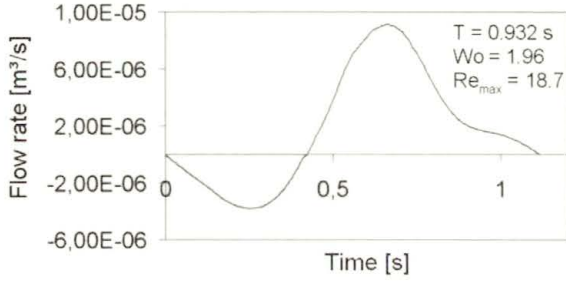

FIGURE 22. Flow curve of the investigated pulsatile flow (T: time period; Wo: Womersley number)

In this case it was not possible to compare the results of the new method with an analytical method. Therefore, the comparison was done with computational fluid dynamics (CFD) results. The CFD was performed with Fluent 6.2 (Fluent Inc., Lebanon, USA) and the preprocessor Gambit™ (Fluent Inc., Lebanon, USA). In Fig. 23 (left) CFD results for two wall distances and for one experiment are depicted. The experimental data was obtained from all

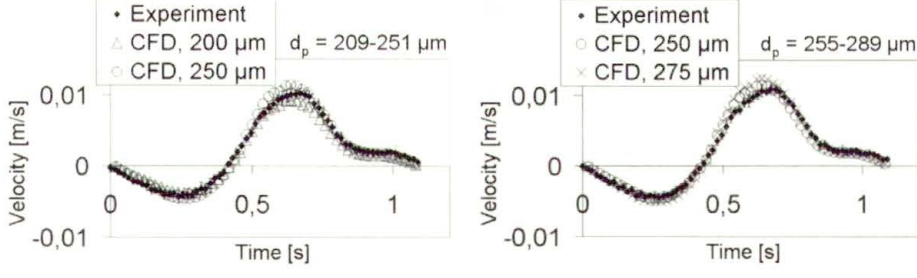

FIGURE 23. Comparison between experimental assessed velocity close to the wall and CFD-results. Left: Experimental velocity obtained from particles with a wall distance d_p between 209 µm and 251 µm. Right: Experimental velocity obtained from particles with a wall distance d_p between 255 µm and 289 µm.

particles with a wall distance between 209 µm and 251 µm. In Fig. 23 (right) the comparison is made for all particles with a wall distance between 255 µm and 289 µm and for CFD results for two wall distances. There is a very good agreement for both wall distance intervals. Note: CFD was validated in the central plane with conventional PIV.

3.3.3. Validation in a complex steady flow with planar walls. To prove the reliability of the new method in more complex flows than in the two sections before, we investigated the flow in an U-shaped duct with a so called backward facing step, see Fig. 24. The cross sections are rectangular. In such a flow model separation zones, reattachment zones, and secondary flow can be observed. To give an impression of the flow in this duct, the path lines for two cross sections are depicted in Fig. 25: a cross section in an x-z plane with the separation in the diagram above, and below in the x-y plane just in the middle of the duct. The impact of the secondary flow can be seen by the deformation of the path lines. The path lines are calculated with CFD.

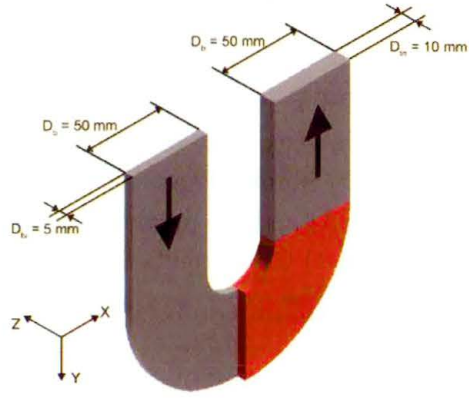

FIGURE 24. Dimensions of U-shaped duct with rectangular cross section, backward-facing step and red-colored investigation section

In Fig. 26 a comparison is depicted between experimentally and numerically obtained velocity vector fields at the wall for Re = 30.1 (Re is calculated with the mean velocity and depth before the step). On the left side, the experimental results for all particles with a wall distance between 223 µm and 250 µm is shown, on the right side the numerically obtained results (again with Fluent) for a wall distance of 240 µm. The reattachment line is clearly visible. The velocity fields show a good agreement. Path lines were calculated from these vector fields, see Fig. 27. The declination of the reattachment line

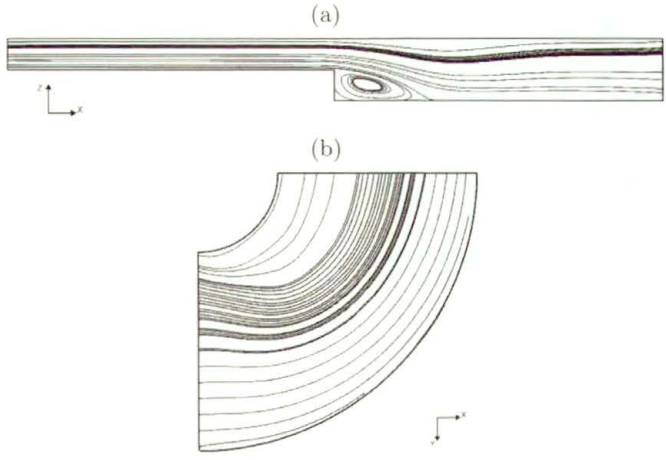

FIGURE 25. Path lines, acquired with CFD, in two cross sections (Re = 50)

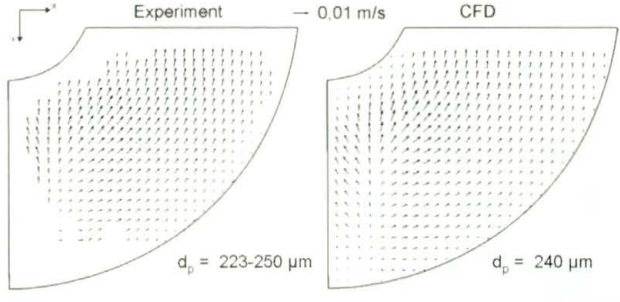

FIGURE 26. Comparison between experimentally and numerically obtained vector fields (Re = 30.1)

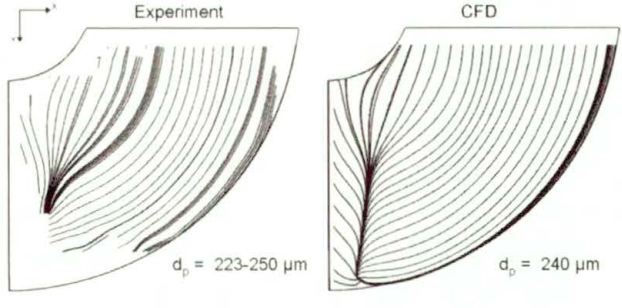

FIGURE 27. Path lines, calculated with the vector fields of Fig. 26 (Re = 30.1)

is visible. Please note, that these path lines are close to the wall, in Fig. 25 the path lines are in center cross sections.

For a quantitative comparison between the experiment and CFD, velocity profiles are considered at different y-positions, see Fig. 28. The comparison can be seen in Fig. 29 for the position y_4. In Fig. 29(left) the experimental results for all particles with a wall distance between 184 µm and 220 µm is shown and compared to CFD calculations of two wall distances. The same is done in Fig. 29(right) for all particles with a wall distance between 223 µm and 250 µm. As expected, the experimental values lie between the CFD results.

In Fig. 30 a comparison of the experimentally and numerically obtained wall shear rate can be seen. The deviation is about 10 %.

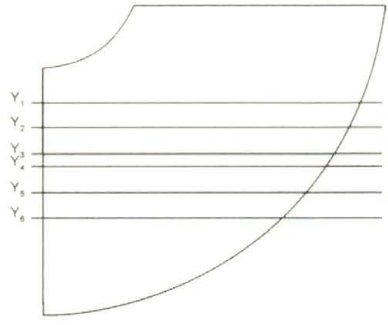

FIGURE 28. Y-positions, where a quantitative comparison between experiment and CFD was done

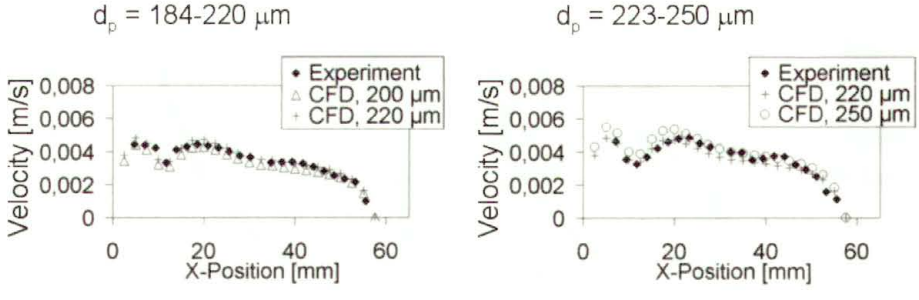

FIGURE 29. Comparison between experimental and numerical results for y_4 and Re = 30.1 for two different experimental wall distance ranges

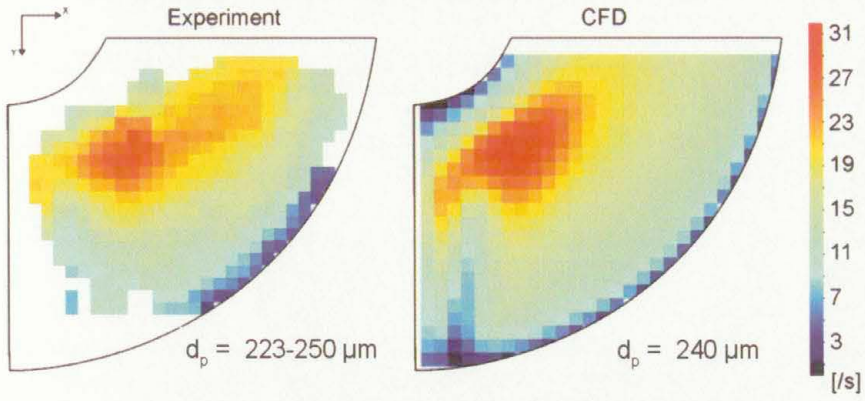

FIGURE 30. Wall shear rate. Experiment on the left side, numerical simulation on the right (Re= 30.1)

3.3.4. Validation in a complex steady flow with vaulted walls. The last validation step is an investigation of a complex flow with vaulted walls. The flow model is similar to before, but with a lenticular cross section, see Fig. 31. To give an impression of the flow in this special duct, depicted in Fig. 32 the path lines for the same two cross sections as in Fig. 25 are used: a cross section in x-z plane with the separation in the diagram above and below in the x-y plane just in the middle of the duct.

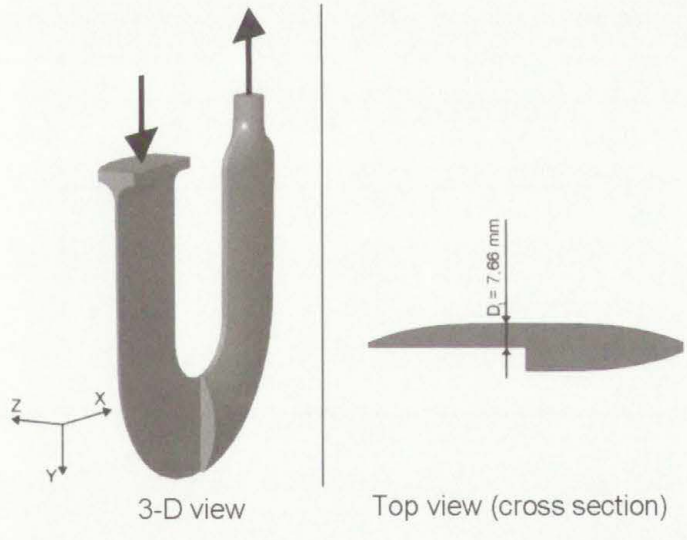

FIGURE 31. U-shaped duct with lenticular cross section and backward-facing step

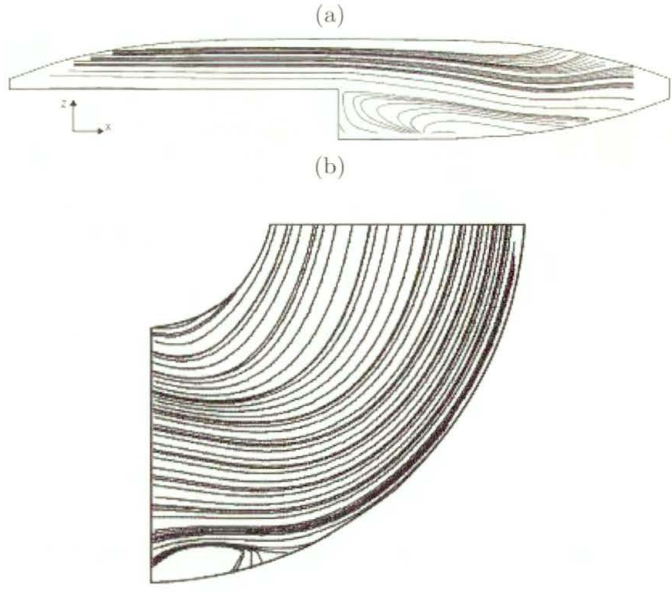

FIGURE 32. Path lines, acquired with CFD, in two cross sections (Re = 50)

As a validation step before a comparison between experimentally and numerically obtained velocity vector fields at the wall is done, see Fig. 33. On the left side, the experimental results for all particles with a wall distance between 230 µm and 270 µm is shown, on the right side the numerically obtained results for a wall distance of 250 µm. The velocity fields show a good agreement. Path lines were calculated out of these vector fields, see Fig. 34. The flow is almost a stagnation point flow.

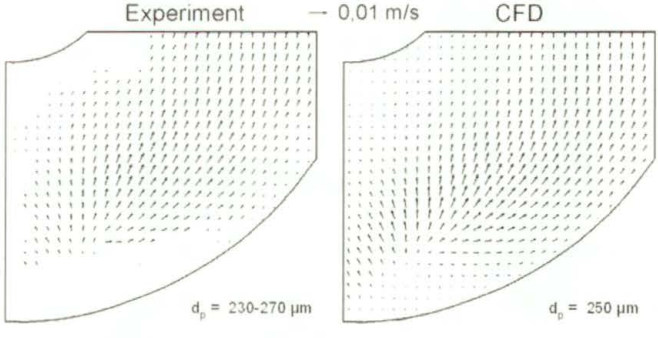

FIGURE 33. Comparison between experimental and numerically obtained vector fields (Re = 36.6)

For a quantitative comparison between the experiment and CFD, velocity profiles at position y_4 (see Fig. 28) are shown in Fig. 35. On the left the experimental results for all particles with a wall distance between 175 µm and 230 µm are shown and compared to CFD calculations of two wall distances. The same is shown in n Fig. 35 (right) for all particles with a wall distance between 230 µm and 270 µm. Despite some deviations, the comparison is quite good.

Again, in Fig. 36 a comparison of the experimentally and numerically obtained wall shear rate can be seen. The deviation in this flow is about 15%.

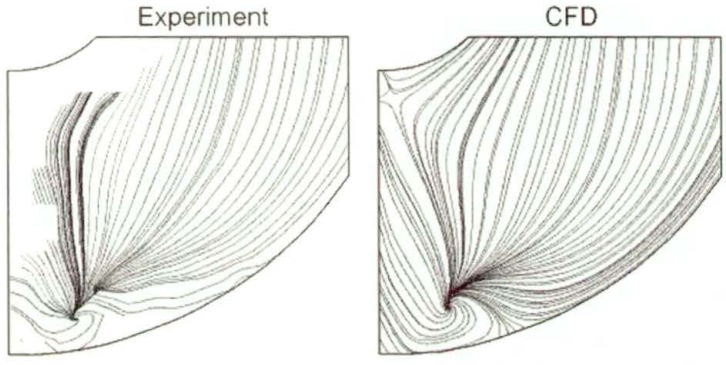

FIGURE 34. Path lines, calculated with the vector fields of Fig. 33 (Re = 36.6 and $d_p = 175 - 230$ µm)

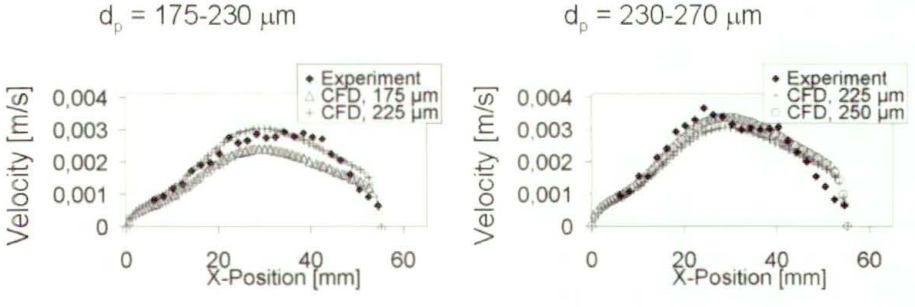

FIGURE 35. Comparison between experimental and numerical results for y_4 and Re = 36.6 (see Fig. 28) for two different experimental wall distance ranges

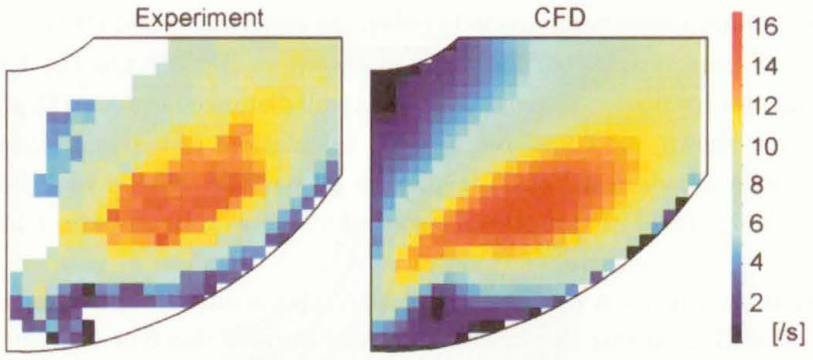

FIGURE 36. Wall shear rate. Experiment on the left side, numerical simulation on the right (Re = 36.6 and $d_p = 175 - 230\,\mu m$)

4. Discussion and Future Work

After a review of different methods to assess the wall shear flow, a new method was presented. This new method is noninvasive, allows the assessment of the wall flow (magnitude, direction and wall distance) with an accuracy of about 10% and is usable in unsteady flows as well as at curved and vaulted surfaces. Reasons for deviations:

- too few particles close to the wall,
- instead of a certain wall distance, a wall distance range is considered,
- migration of particles perpendicular to the wall.

In addition, the size of particles should be minimized. However, despite their size, the results showed that it is possible to assess flow structures accurately. It was necessary to find a compromise between light scattering properties, neutral buoyancy, quality of monodispersity and financial restrictions. Nevertheless, we plan to manufacture smaller particles with a diameter of 100 µm without negatively affecting the monodispersity and keeping the same scattering properties as the bigger beads.

Future work will comprise of:

- flow assessment at rigid but arbitarily vaulted walls (methods from cartography will be used),
- assessment of the third velocity component through using the method of optical flow,
- flow assessment at flexible walls.

References

1. T. ASAKURA and T. KARINO, *Flow patterns and spatial distribution of atherosclerotic lesions in human coronary arteries*, Circ. Res., **66**: 1045–1066, 1990.

2. T. BENCIC, *Pressure-sensitive paint research at GRC*, NASA Glenn Research Center, Optical Instrumentation Technology Branch, `http://www.grc.nasa.gov/WWW/OptInstr/resources/insights.pdf` (July 2005).

3. J. CZARSKE, L. BÜTTNER, T. RAZIK, H. MÜLLER, D. DOPHEIDE, S. BECKER and F. DURST, *Spatial-resolved velocity measurements of shear flows with a novel differential Doppler velocity profile sensor*, `http://in3.dem.ist.utl.pt/lxlaser2002/papers/paper_21_1.pdf` (July 2005).

4. DANTEC DYNAMICS, *Laser Doppler Velocimetry*, `http://www.dantecdynamics.com/LDA/Princip/LDA_principle.jpg` (July 2005).

5. C. HEINZEN, *Herstellung von mikrodispersen Mikrokugeln durch Hydroprilling*, Dissertation, Eidgenössische Technische Hochschule Zürich (1996).

6. M.H. KROLL, J.D. HELLUMS, L.V. MCINTIRE, A.I. SCHAFER and J.L. MOAKE, *Platelets and shear stress*, Blood, **88**: 1525–1541, 1996.

7. LAVISION, *System Components for Particle Image Velocimetry*, `http://www.piv.de/graphics/pivsetup.jpg` (July 2005).

8. H. MENG, *Tackling turbulence with holographic particle image velocimetry*, AIAA Fluid Dynamics Conference, 30 th, Norfolk, VA, 1999, `http://www.eng.buffalo.edu/Departments/mae/LFD/publications/1999/1999-2.pdf` (July 2005).

9. W. MORTON and R. CUMMING, *A technique for the elucidation of Virchowfs Triad*, Ann NY Acad Sci, **283**, p.477, 1977.

10. R.M. NEREM, R.W. ALEXANDER, D.C. CHAPPELL, R.M. MEDFORD, S.E. VARNER and W.R. TAYLOR, *The study of the influence of flow on vascular endothelial biology*, Am. J. Med. Sci., **316**(3): 169–175, 1989.

11. G.P. NOON, *Clinical use of cardiac assist devices*, [in:] T. Akutsu, K. Koyanagi [eds.], Heart Replacement—Artificial Heart **4**, pp.195–204, Springer Verlag, 1993.

12. H. PARK, J. A. MOORE, O. TRASS and M. OJHA, *Laser photochromic velocimetry estimation of the vorticity and pressure field $\tilde{U}$ two-dimensional flow in a curved vessel*, Experiments in Fluids 26 (1999).

13. B. RUCK, *Statische-scannende Systeme*, GALA e. V., `http://www.gala-ev.de/images/Stat-Scan-Anordnung.jpg` (July 2005).

14. SIGNAL PROCESSING SA, *Ultrasonic Doppler velocimetry*, `http://www.signal-processing.com/images/devices/working_principle.gif` (July 2005).

15. M. TRIEP, CH. BRÜCKER and W. SCHRÖDER, *Visualization and high-speed PIV measurements of the flow downstream a dynamic mechanical model of the human vocal folds*, Aerodynamisches Institut der RWTH Aachen, `http://in3.dem.ist.utl.pt/lxlaser2004/pdf/paper_23_1.pdf` (July 2005).

16. E. ZANOUN, *Oil Film Interferometry for Wall Shear Stress Measurements*, LAS – BTU Cottbus, `http://www.tu-cottbus.de/LAS/images/D4-1.gif` (July 2005).